Journal of Renewable Energy and Sustainable Development (RESD) Volume 9, Issue 2, December 2023 - ISSN 2356-8569
http://dx.doi.org/10.21622/RESD.2023.09.2.042

Received on, 09 September 2023 Accepted on, 29 November 2023 Published on, 20 December

Computational Simulation Study of the Impact of Isotropic GDL Thermal Conductivity on PEMFC Characteristics

Mahmut Kaplan

Department of Machine and Metal Technology, Naci Topcuoglu Vocational High School, Gaziantep University, Gaziantep, Turkey

mahmutkaplan@gantep.edu.tr

ABSTRACT

The technical capability of proton exchange membrane fuel cell (PEMFC) offers an encouraging solution to produce sustainable and clean power. The gas diffusion layer (GDL) is a pivotal part of the PEMFC which plays a critical role in providing a pathway for reactant and product. GDL electrically connects the catalyst layer to the current collector and conducts heat generated in the electrochemical reactions. The thermal conductivity is one of the most important transport properties of the GDL that affects heat transfer across the cell and the overall performance. In the current work, the impact of the isotropic GDL thermal conductivity ranging 1-100 W/mK at 0.4 and 0.6 V on the cell efficiency is studied computationally using ANSYS Fluent PEMFC module. The results indicate that an increase in the isotropic GDL thermal conductivity enhances the fuel cell current density considerably up to 20 W/mK with the more homogeneous temperature distribution and lower temperature across PEMFC at 0.4 and 0.6 V. After this, the impact of the GDL thermal conductivity on the performance diminishes and thus the current density is nearly constant with further increase in isotropic GDL thermal conductivity at both cell voltages. The peak current density of 1.37 A/cm2 is gained at 100 W/mK. The power function provided a good fit with the calculated data. Oxygen consumption and water production augments with higher thermal conductivity, especially the regions above the cathode current collector ribs.

Index-words: *PEMFC, GDL, Thermal conductivity, Heat transfer, Performance; CFD.*

I. INTRODUCTION

Internal combustion engines are widely applied to a power source for commercial and passenger vehicles over the past decades. They consume carbon-based fossil fuels (gas or diesel) which are the non-renewable energy sources producing significant pollutants such as greenhouse gasses (CO_2, CH_4, and N_2O), hazardous gases (CO, and NO_x) and particulate matter. Their extensive use leads to degrading the air quality, detrimental health problems and climate change. The largest chunk of greenhouse gas is owing to CO_2 production accounted for 76% of the emitted global greenhouse gases in 2010 (Towoju and Ishola, 2020). Therefore, in the last two decades, alternative power sources such as hydrogen energy systems have been improved to solve problems (Dincer, 2008; Barbir, 2013). A fuel cell as an electrochemical energy converter is one of the of the most encouraging alternative energy sources of the future. It produces quiet, efficient and clean electricity. Proton exchange membrane fuel cell (PEMFC) is the most distributed cell type owing to having low-temperature operation, modularity, light weight and being suited for a variety of applications including portable power, backup power and automotive applications (Spiegel, 2008). A PEMFC is a multi-component device containing a membrane-electrode assembly (MEA) and current collectors having flow channels machined. The MEA is comprised of anode and cathode catalyst layer (CL) and gas diffusion layer (GDL) being separated by a polymer membrane. The oxidation and reduction reactions occur inside the anode and cathode CL, respectively. Hydrogen is broken down into protons and electrons at the anode CL. Protons travel throughout the PEMFC whereas electrons move via an external circuit toward the cathode. They react with oxygen, and as a result the electricity, water and waste heat are produced at the cathode CL. GDLs being the outermost layers of the MEA serve to transport of water, electrons and heat generated in the cell reactions from CL to bipolar plates (Cindrellaa et al., 2009). Besides, GDL as a porous medium provides a pathway for reactants from the gas channel to CL and mechanical support to the MEA (Okonkwo and Otor, 2021). GDL properties such as porosity, diffusivity, permeability, electrical and thermal conductivity affect transport behaviour of PEMFC (Athanasaki et al., 2023). Thermal conductivity as a significant GDL transport property plays a dominant role in the temperature distribution of PEMFC and moving heat by the diffusion (Omrani and Shabani, 2019). The waste heat induced throughout the cathode reaction at the CL is a primary heat source affecting the temperature distribution of PEMFC. The heat can be taken away from the cell by conduction (solid structure) and convection (species flow).

Besides, the reactant gases and product water discharge the residual heat into the environment (Zamel and Li, 2013). In the bipolar plates connected electrodes by GDLs, the heat is dissipated by both conduction and convection owing to their embedded flow channels. Since the bipolar plates have higher thermal conductivity compared with that of the gases in the channels, heat can be easily taken away from the plates. That is, the heat transfer from the GDL region close to gas channels is lower than the region close to the lands. Therefore, GDL thermal conductivity strongly affects temperature distribution and heat removal capability of PEMFC. Turkmen et al. (2023) calculated the GDL thermal conductivity under various working temperatures (20-80 °C). It was concluded that high cell temperature had a positive impact on the thermal conductivity in the electrodes. They also suggested several correlations (polynomial, rational and power) to express the thermal conductivity depending on the temperature.

In literature (He et al., 2010; Alhazmi, 2013; Chowdhury et al., 2016; Alcántara, 2022) and a variety of computational and experimental investigations have been carried out to understand the influence of GDL thermal conductivity on PEMFC performance. He et al. (2010) improved a two-phase, three-dimension model to scrutinize the impact of the anisotropy of GDL thermal conductivity along the x, y and z directions on the water and heat management. The results demonstrated that compared to isotropic GDL, larger temperature difference was produced by the anisotropic GDL, especially the in-plane conductivity perpendicular to the gas channels, which led to the reduction in the current density and non-uniform water saturation compared to the isotropic case. Alhazmi et al. (2013) examined the effects of anisotropic GDL thermal conductivity on the performance at various operating temperatures for both through-plane (1-10 W/mK) and in-plane (1-100 W/mK) directions using the PEMFC module of ANSYS FLUENT. They found that a rise in the in-plane and through-plane thermal conductivity resulted in significantly higher power density of PEMFC. They also reported that the temperature gradients and maximum temperature in PEMFC decreased when increasing GDL thermal conductivity in both directions.

Alcántara et al. (2022) studied the influence of the distinct GDL transport features on the performance employing the CFD software ANSYS FLUENT and they reported that lower GDL thermal conductivity led to high temperatures and temperature gradients in the membrane. The temperature gradient is a key parameter that affects both heat and water transfer in PEMFC and thus the long-term stability and durability of the cell components (Ozden, 2019).

Based on the literature, it is concluded the GDL thermal conductivity influences the temperature difference in the PEMFC and thus the performance characteristics. Temperature distribution through GDL influences water and heat transport mechanisms, and hence the durability of PEMFC parts. The anisotropic GDL augments the temperature variation and results in more non-uniform current density compared to the isotropic GDL. There are a lot of studies related to the effect of anisotropic GDL on heat transfer and PEMFC performance. But there is not enough information available on the interactions between the isotropic GDL thermal conductivity, gas species concentrations and temperature distribution through the components.

The current work aims to study the influence of the isotropic thermal conductivity of the GDL on the temperature, oxygen and water distribution inside the porous layers and the cell performance. The findings of this research study can be beneficial to researchers, designers, and engineers for improving design and performance of the PEMFC system.

II. METHODS AND MATERIALS

A. CFD Model and Operating Parameters

In this computational study, the PEMFC geometry is adopted from Wang et al.'s (2003) experiment. The length and width of the fuel cell are 0.07 and 0.002 m, respectively. The electrolyte projected area is specified as 0.00014 m^2. The height and width of gas channels are 0.01 m. The CLs, GDLs, and membrane thicknesses are 1.29×10^{-5}, 3×10^{-4} and 1.08×10^{-4} m, respectively (Kaplan, 2022a).

The operating characteristics of the model are provided in Table I. Thermal conductivity of the components is given in Table II.

TABLE I: OPERATING FEATURES OF PEMFC.

Parameter	Value
Temperature of the cell	343 K
Open circuit potential of the cell	0.94 V
Reference exchange current density (anode and cathode)	4000 and 0.1 A/m^2
Inlet mass flow rate (anode and cathode)	5.40 x 10^{-6} and 3.29 x 10^{-5} kg/s
Inlet H_2 and H_2O mass fraction (anode)	0.2 and 0.8 (Kaplan, 2022b)
Inlet O_2 and H_2O mass fraction (cathode)	0.2 and 0.1 (Kaplan, 2022b)
H_2O and H_2 reference diffusivity	7.33 x 10^{-5} m^2/s (Biyikoglu and Alpat, 2011)
O_2 and other species reference diffusivity	2.13 x 10^{-5} and 4.9 x 10^{-5}m^2/s
Porosity and viscous resistance GDL and CL	0.5 and 1 x 10^{12} 1/m^2 (Kahveci and Taymaz, 2018)
Surface/volume ratio of CL	200000 1/m
Anodic and cathodic transfer coefficient at anode and cathode	0.5 and 2 (Wang et al., 2003)

TABLE 2: THERMAL CONDUCTIVITY OF CELL COMPONENTS.

Components	Value
Bipolar plate	100 W/mK
GDL	1-100 W/mK
CL	10 W/mK
Membrane	2 W/mK

B. Assumptions

The assumptions employed in the current 3D PEMFC model are:

- The calculation process of PEMFC is under the steady state condition.
- The flow is laminar and incompressible.
- The gas species are supposed to be as perfect gases.
- The MEA are regarded as isotropic and homogenous porous medium.
- Contact resistance between different layers is neglected.
- Gas cross-over through the membran is ignored.

C. Conservation Equations

The following conservation equations govern physical phenomena occurring within a PEMFC:

$$\nabla(\rho\vec{u}) = 0 \quad (1)$$

$$\frac{1}{(\varepsilon)^2}\nabla(\rho\vec{u}\vec{u}) = -\nabla P + \nabla(\tau) + S_m \quad (2)$$

$$\nabla(\vec{u}C_i) = \nabla(D_i^{eff}\nabla C_i) + S_i \quad (3)$$

$$\nabla(\rho c_p\vec{u}T) = \nabla(k^{eff}\nabla T) + S_e \quad (4)$$

$$\nabla\left(\sigma_{mem}\nabla\phi_{mem}\right) + R_{mem} = 0,\ \nabla\left(\sigma_{sol}\nabla\phi_{sol}\right) + R_{sol} = 0 \quad (5)$$

$\vec{u}$ and ρ are the velocity vector and density of species. ε is the porosity of porous media. P and τ are the species pressure and viscous stress tensor. C_i and D_i^{eff} are the species (i) mass fraction and effective diffusion coefficient. c_p and k_{eff} the constant-pressure heat capacity and effective thermal conductivity. T is the temperature. R_{mem}, φ_{mem}, σ_{mem} and R_{sol}, φ_{sol}, σ_{sol} are the volumetric transfer current, electric potential and electrical conductivity of membrane and solid electrode, respectively. S_m, S_i and S_e are the source terms of the momentum, species and energy, respectively.

D. Boundary Conditions

On the inlet and outlet faces of the gas channels, the fixed mass flow rate and pressure boundary conditions are imposed, respectively. All other surfaces are the no-slip with zero flux wall boundary conditions. The surfaces of the current collectors are represented as the anode and cathode terminals on which their potentials are set to 0 V and 0.4-1 V, respectively, for drawing the polarization curve. The temperature of inlet fuel and air is 343 K.

E. Numerical Methodology

All parts of the geometry required to ANSYS Fluent Fuel Cell Module (ANSYS, 2013) are created and assembled using SOLIDWORKS software. The structured hexahedral mesh is generated for each component of

PEMFC using the sweep method in ANSYS Meshing in Figure 1. The modelling domain involves 1254400 cells obtained by the grid independence test in a previous study (Kaplan, 2021). The governing equations used in the present computations are solved with pressure-based solver algorithms based on finite volume method in CFD software ANSYS Fluent. The SIMPLE algorithm is chosen as a solver scheme. The Least Squares Cell Based discretization method is selected for the gradient. The Second Order discretization scheme is employed for pressure, momentum, density and species.

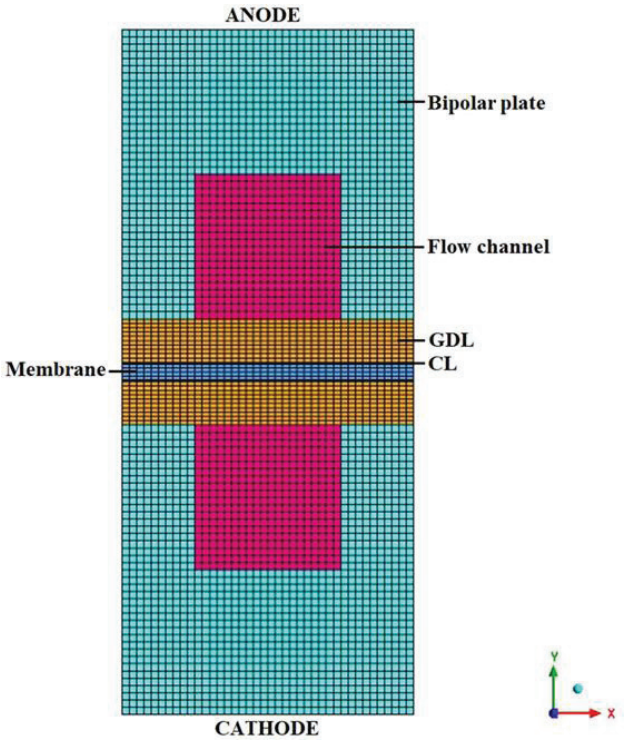

Fig 1. Meshed computational domain of PEMFC model

F. Model Validation

In the present work, the CFD model validation is conducted using the measured data (Wang et al., 2003) in Figure 2. It is seen that the polarization curve demonstrates good agreement with the measured data, particularly at low and medium current densities. The overprediction is seen at high current densities. The most probably reason for this is that the present model disregards the liquid water presence inside the porous layers leading to a decrease in porosity of the layers and a rise in species mass transfer resistance.

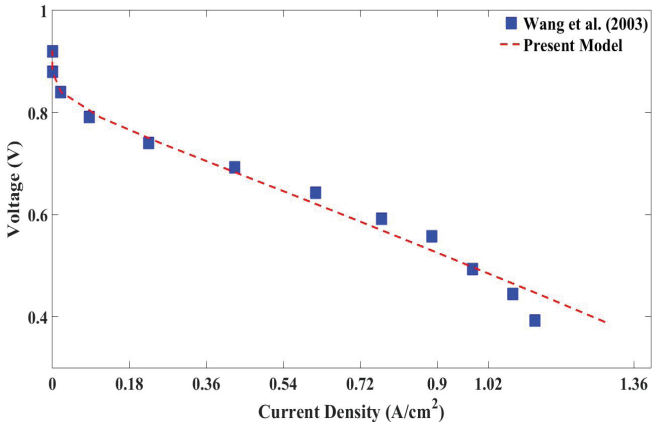

Fig 2. Polarisation curve for the numerical predictions compared with the measured data

III. RESULTS AND DISCUSSION

The present study focuses on examining the influence of the isotropic GDL thermal conductivity on the performance characteristics of PEMFC. Figure 3 indicates the cell current density versus GDL thermal conductivity (1-100 W/mK) plots at 0.4 and 0.6 V. The current density shows the same trend at both cell voltages in Figure 3: a rise with increasing the GDL thermal conductivity.

The influence of GDL thermal conductivity on PEMFC performance diminishes after 20 W/mK and the current density is almost constant with further increase in isotropic GDL thermal conductivity.

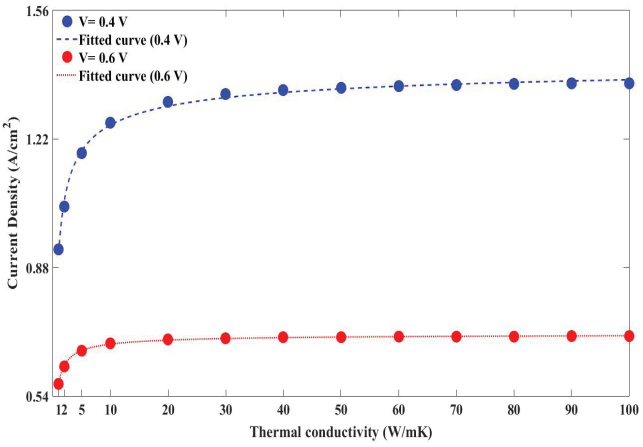

Fig 3. Current density versus GDL thermal conductivity plot at 0.4 and 0.6 V

Türkmen et al. (2023) experimentally examined the influence of temperature change on the GDL thermal conductivity and they reported that the power type correlation was the most suitable to describe thermal conductivity evaluated as a function of the measured temperature. Similar to Türkmen et al. (2023), the calculated data points are fitted to a power function of the form as:

$$I = ak^b + c \quad (5)$$

where I is current density and k is the GDL thermal conductivity. a, b and c are coefficients in Equation (5) which are determined using the MATLAB Curve Fitting Toolbox. a = –0.5243, b = –0.452 and c = 1.442 at 0.4 V. a = –0.1345, b = –0.6798 and c = 0.7054 at 0.6 V. The R-square value of the power function at 0.4 and 0.6 V is 0.99 with a 95% confidence bound. Fitted curves for 0.4 and 0.6 V in Figure 3 are shown by dashed and dotted lines, respectively.

It is clear in Figure 3 that the maximum current density is achieved with the GDL thermal conductivity of 100 W/mK at 0.4 V. As is evident in Figure 3, an increase in the GDL thermal conductivity from 1-10 to 100 W/m K leads to an improvement of the current density of the PEMFC from 0.92-1.26 to 1.37 A/cm^2, respectively. In the following sections, the impact of different isotropic GDL thermal conductivities (1, 10 and 100 W/mK) on the distribution of temperature, oxygen and water in the PEMFC is examined at 0.4 V.

A. Influence of the GDL Thermal Conductivity on the Cell Temperature

Figure 4 illustrates the temperature distribution for two different cathode GDL regions: near the CL and near the flow channel (NCL and NFC) for thermal conductivities of 1, 10 and 100 W/mK at 0.4 V.

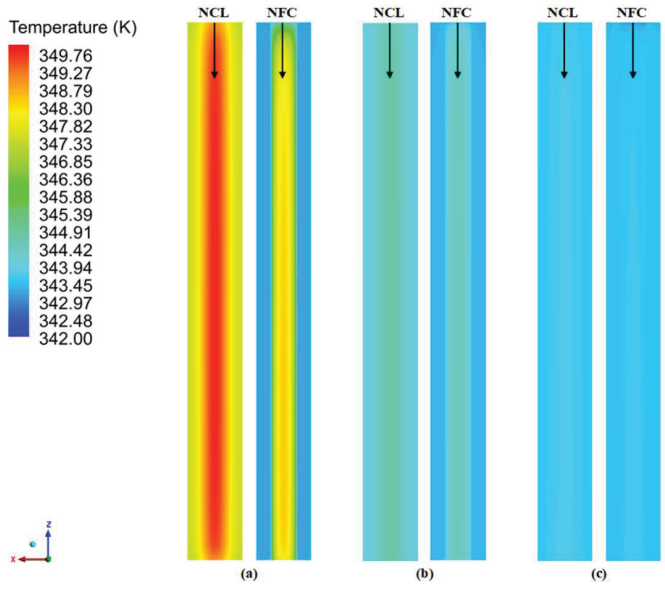

Fig 4. Influence of GDL thermal conductivity on temperature distribution in two regions close to CL and close to flow channel at (a) 1 W/mK, (b) 10 W/mK, and (c) 100 W/mK

It is seen in Figure 4 that an increase in the GDL thermal conductivity decreases temperature in two selected GDL regions. The sensitivity of the temperature gradient in the selected regions diminishes with higher GDL thermal conductivity. of PCM The maximum temperature of 349.76 K is observed near the CL region at 1 W/mK due to heat transfer rate being poor at low GDL thermal conductivity in Figure 4a.

Temperature decreases towards the flow channel at 1, 10 and 100 W/mK in Figure 4. Meanwhile, temperature above the land regions is lower than that above the flow channel, especially at 1 and 10 W/mK due to bipolar plate thermal conductivity being higher than that of the gas species. Besides, temperature homogeneity enhances remarkably with the GDL thermal conductivity of 100 W/mK in Figure 4c.

Figure 5 shows temperature distribution along to lateral direction at the inlet and outlet of the middle of cathode GDL thickness for various GDL thermal conductivities. An increase the GDL thermal conductivity results in decreasing temperature at the inlet and outlet in Figure 5.

Besides, temperature at the outlet is higher than the inlet temperature in Figure 5. However, temperature difference between inlet and outlet decreases with increasing thermal conductivity from 1 to 100 W/mK. It is found that temperature distribution over the mid-thickness of cathode GDL is more uniform at 100W/mK in Figure 5.

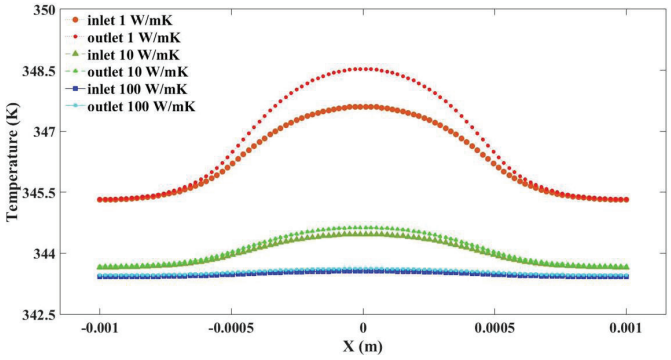

Fig 5. Comparison of lateral temperature distribution at the inlet and outlet of mid-thickness of GDL for different GDL thermal conductivities

Figure 6 shows temperature distribution at the middle of the cell length for GDL thermal conductivities of 1, 10 and 100 W/mK. As illustrated in Figure 6, temperature through the MEA is very high and non-uniform at 1 W/mK.

The elevated temperature in PEMFC leads to a dry membrane which reduces protonic conductivity through the cell and facilitates the membrane fracture. An increase in the GDL thermal conductivity from 1 to 100 W/mK leads to more homogeneous temperature distribution and lower temperature throughout PEMFC in Figure 6. It is concluded that augmenting GDL thermal conductivity results in a decrease in the temperature gradient and an enhancement in temperature homogeneity thoroughly the cell.

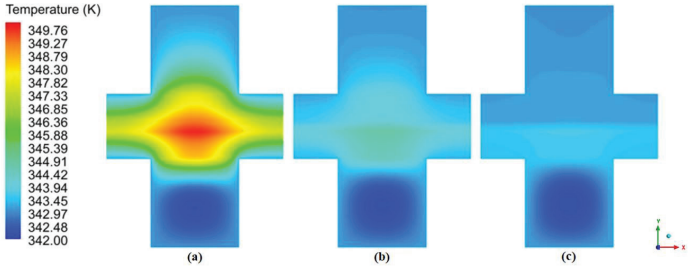

Fig 6. Comparison of temperature distribution at the middle of the cell length for three different GDL thermal conductivities: a) 1 W/mK, b) 10 W/mK, and c) 100 W/mK at 0.4 V

B. Influence of the GDL Thermal Conductivity On the Oxygen and Water Concentration

Figure 7 shows the oxygen concentration distributions of two cathode GDL regions: close to the CL and close to the channel for various thermal conductivities of 1, 10 and 100 W/mK at 0.4 V.

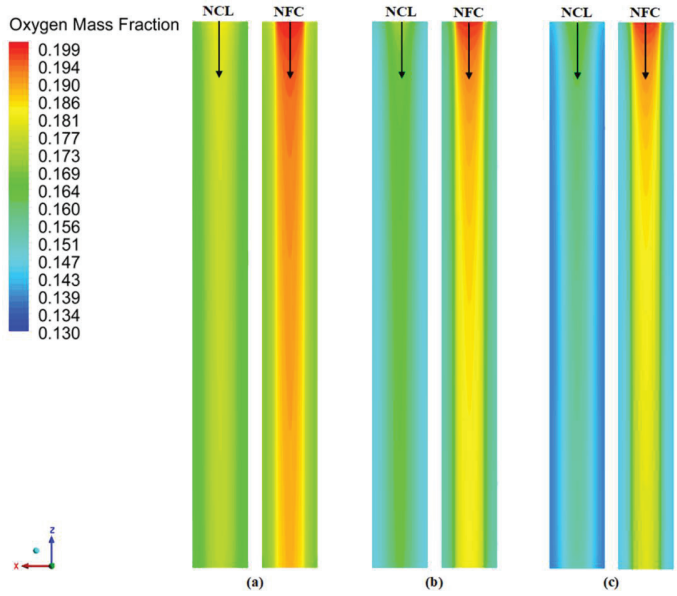

Fig 7. Influence of GDL thermal conductivity on oxygen distribution in two regions close to CL and close to flow channel at (a) 1 W/mK, (b) 10 W/mK, and (c) 100 W/mK

There is a significant correlation between enhanced current density obtained with higher GDL thermal conductivity and oxygen consumption in the GDL in Figure 7. The trend is clear that the oxygen mass fraction reduces significantly when the GDL thermal conductivity elevates from 1 to 100 W/mK for two regions. As illustrated in Figure 7c, the maximum oxygen consumption is obtained with a GDL thermal conductivity of 100 W/mK in the region near the cathode CL where the hydrogen/oxygen reaction occurs. Besides, the amount of oxygen in the region above the flow channel is higher than in the regions above the bipolar plate because of the rib regions not directly connected to the flow channels and suffering from a slow oxygen mass transfer. Figure 8 shows comparison of lateral oxygen distribution at the inlet and outlet of mid-thickness of GDL for various GDL thermal conductivities.

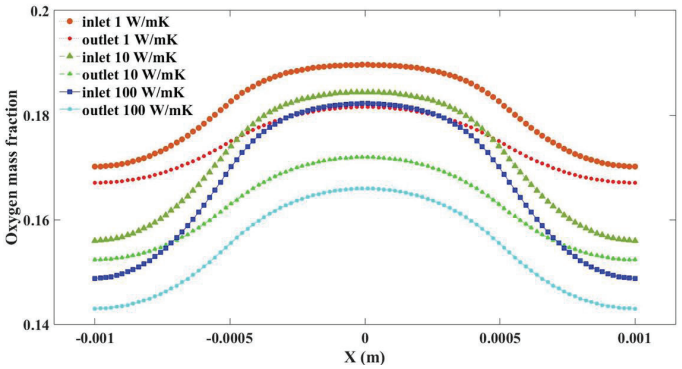

Fig 8. Comparison of lateral oxygen distribution at the inlet and outlet of mid-thickness of GDL for different GDL thermal conductivities

Oxygen mass fraction decreases from inlet to outlet owing to oxygen diffusion into the cathode CL in Figure 8. Besides, an increase in GDL thermal conductivity from 1 to 100 W/mK leads to lower oxygen concentration for two regions. Similar to Figure 7, the maximum oxygen mass fraction is detected in the region above the channel.

Figure 9 demonstrates oxygen concentration contour in the cathode channel, GDL and CL at a midway location between inlet and outlet. A strong decrease of oxygen in the cathode CL and GDL is observed as the thermal conductivity increases from 1 to 100 W/mK at 0.4 V in Figure 9. It is clear that the higher oxygen concentration is detected in the region above the channel whereas it is remarkably lower in the regions above the lands where they are not directly exposed to the channels in Figure 9.

Figure 10 demonstrates the water concentration distributions of two regions: close to CL and close to the channel for different thermal conductivities (1-100 W/mK) at 0.4 V. There is an opposite relation between water and oxygen mass fraction.

Unlike the oxygen mass fraction in Figure 7, the water mass fraction enhances remarkably when the GDL thermal conductivity increases from 1 to 100 W/mK in Figure 9. It is clear in Figure 10c that the maximum water production is achieved at 100 W/mK in the region near the cathode CL due to the electrochemical reaction.

An increase in water generation with higher GDL thermal conductivity results in more hydrated membrane and reduction of ohmic loss. Besides, the water concentration augments in the regions above the lands because of higher oxygen consumption there.

Volume 9, Issue 2, December 2023 - ISSN 2356-8569
http://dx.doi.org/10.21622/RESD.2023.09.2.042

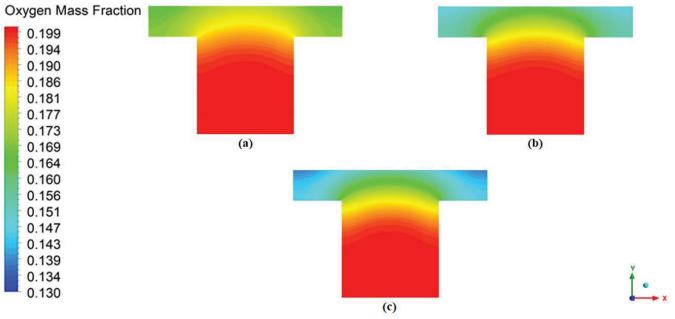

Fig 9. Oxygen distribution throughout cathode CL, GDL and flow channel for three different GDL thermal conductivities: a) 1 W/mK, b) 10 W/mK, and c) 100 W/mK at 0.4 V

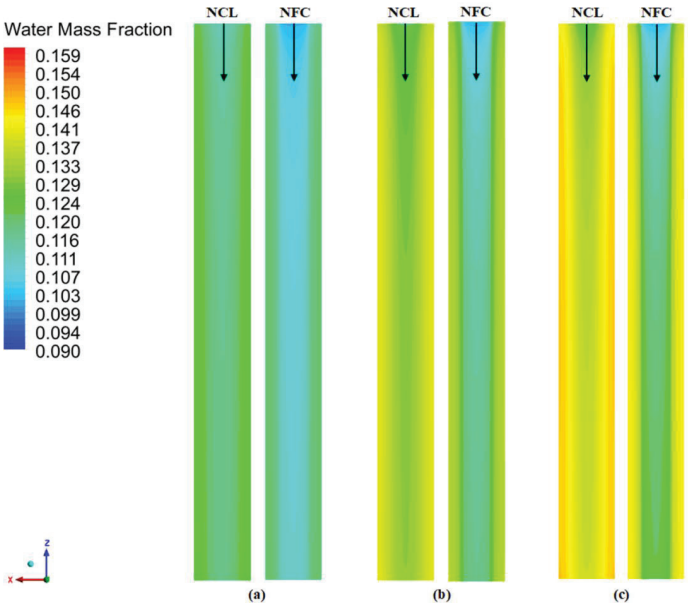

Fig 10. Influence of GDL thermal conductivity on water distribution in two regions close to CL and close to flow channel at (a) 1 W/mK, (b) 10 W/mK and (c) 100 W/mK

Figure 11 demonstrates comparison of water distribution at the inlet and outlet of mid-thickness of GDL for various thermal conductivities. The mass fraction of water increases gradually from inlet to outlet due to water produced by the cathode reaction in Figure 11.

Figure 12 indicates water concentration contour in the cathode channel, GDL and CL at a midway location between inlet and outlet. A strong increase of water mass fraction in the CL and GDL is observed as the thermal conductivity increases from 1 to 100 W/Mk in Figure 12. In addition, the water removal from the GDL is higher in the region above the gas channel compared with that in the regions above the ribs because of the channel allowing direct contact of water to the GDL.

The results show that higher GDL thermal conductivity leads to reducing oxygen concentration and augmenting water concentration in both the lateral and longitudinal directions.

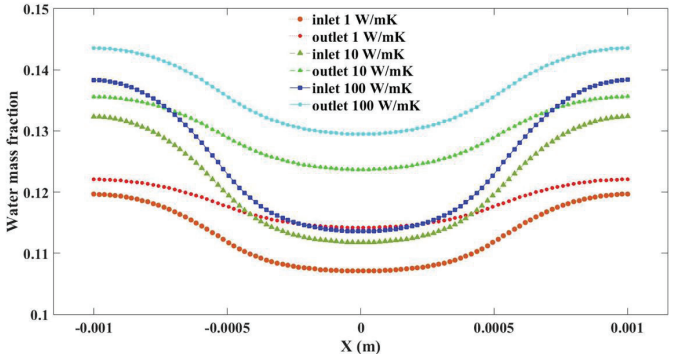

Fig 11. Comparison of lateral water distribution at the inlet and outlet of mid-thickness of GDL for different GDL thermal conductivities

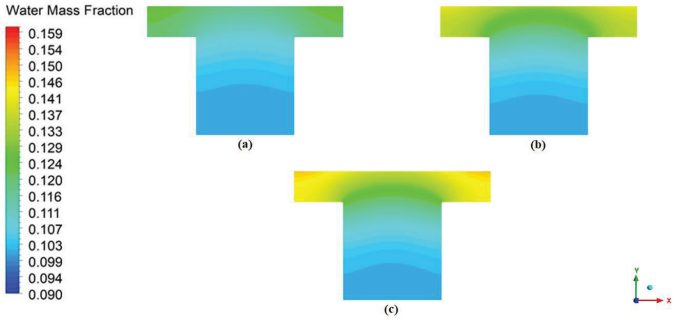

Fig 12. Water distribution throughout cathode CL, GDL and flow channel for three different GDL thermal conductivities: a) 1 W/mK, b) 10 W/mK, and c) 100 W/mK at 0.4 V

IV. CONCLUSIONS

In the current work, the impact of GDL thermal conductivity on PEMFC performance is scrutinized by CFD method. The results show that:

- The power function is a good fit to the calculated current density data obtained at 1-100 W/mK.
- Elevating isotropic GDL thermal conductivity results in temperature gradient reduction and more homogeneous temperature distribution in the cell.
- The water mass fraction intensifies in the regions above the ribs of the cathode current collector thanks to higher oxygen consumption there.
- The increased hydration with higher isotropic thermal conductivity improves the proton conductivity of the membrane and PEMFC performance.
- The PEMFC performance enhanced with higher thermal conductivity of GDL. But the impact of GDL thermal conductivity on PEMFC performance decreases after 20 W/mK and the current density is nearly fixed with further increase in isotropic GDL thermal conductivity at 0.4 and 0.6 V. This is due to increase in thermal conductivity from 1 to 20 W/mK leads to a reduction in temperature difference thanks to heat removal from the cell and thus almost uniform temperature distribution along the GDL.

These outcomes provide key insights for improving the design and performance of PEMFC, which are pivotal for the commercialisation of PEMFC technology and diverse applications including portable power and automotive applications.

V. References

[1] N. Zamel and X. Li, "Effective transport properties for polymer electrolyte membrane fuel cells e with a focus on the gas diffusion layer," *Prog Energy Combust Sci*, vol. 39, pp. 0–39, 2013.

[2] G. Wei, C. Wang, C. Jiang, and J. Zhang, "The Investigation of Flow Channel Design on the Performance of PEM Fuel Cell," *ECS Meeting Abstracts*, vol. MA2017-01, no. 22, 2017, doi: 10.1149/ma2017-01/22/1133.

[3] A. Can Turkmen, M. Espinoza-Andaluz, C. Celik, B. Sunden, and H. Serhad Soyhan, "Impact of the temperature variation on the thermal conductivity of gas diffusion layers for polymer electrolyte fuel cells," *Fuel*, vol. 345, 2023, doi: 10.1016/j.fuel.2023.128097.

[4] O. A. Towoju and F. A. Ishola, "A case for the internal combustion engine powered vehicle," in *Energy Reports*, 2020. doi: 10.1016/j.egyr.2019.11.082.

[5] A. Ozden, S. Shahgaldi, X. Li, and F. Hamdullahpur, "A review of gas diffusion layers for proton exchange membrane fuel cells—With a focus on characteristics, characterization techniques, materials and designs," *Progress in Energy and Combustion Science*, vol. 74. 2019. doi: 10.1016/j.pecs.2019.05.002.

[6] R. Omrani and B. Shabani, "Review of gas diffusion layer for proton exchange membrane-based technologies with a focus on unitised regenerative fuel cells," *International Journal of Hydrogen Energy*, vol. 44, no. 7. 2019. doi: 10.1016/j.ijhydene.2018.12.120.

[7] P. C. Okonkwo and C. Otor, "A review of gas diffusion layer properties and water management in proton exchange membrane fuel cell system," *International Journal of Energy Research*, vol. 45, no. 3. 2021. doi: 10.1002/er.6227.

[8] M. Kaplan, "Three-dimensional CFD analysis of PEMFC with different membrane thicknesses," *Renewable Energy and Sustainable Development*, vol. 8, no. 2, 2022, doi: 10.21622/resd.2022.08.2.045.

[9] mahmut kaplan, "A Numerical Parametric Study on the Impacts of Mass Fractions of Gas Species on PEMFC Performance," *SSRN Electronic Journal*, 2023, doi: 10.2139/ssrn.4222199.

[10] G. He, Y. Yamazaki, and A. Abudula, "A three-dimensional analysis of the effect of anisotropic gas diffusion layer(GDL) thermal conductivity on the heat transfer and two-phase behavior in a proton exchange membrane fuel cell(PEMFC)," *J Power Sources*, vol. 195, no. 6, 2010, doi: 10.1016/j.jpowsour.2009.09.059.

[11] I. Dincer, "Hydrogen and Fuel Cell Technologies for Sustainable Future," *Jordan Journal of Mechanical and Industrial Engineering*, vol. 2, no. 1, 2008.

[12] L. Cindrella *et al.*, "Gas diffusion layer for proton exchange membrane fuel cells-A review," *Journal of Power Sources*, vol. 194, no. 1. 2009. doi: 10.1016/j.jpowsour.2009.04.005.

[13] A. Vikram, P. R. Chowdhury, R. K. Phillips, and M. Hoorfar, "Measurement of effective bulk and contact resistance of gas diffusion layer under inhomogeneous compression - Part I: Electrical conductivity," *J Power Sources*, vol. 320, 2016, doi: 10.1016/j.jpowsour.2016.04.110.

[14] G. Athanasaki, A. Jayakumar, and A. M. Kannan, "Gas diffusion layers for PEM fuel cells: Materials, properties and manufacturing – A review," *International Journal of Hydrogen Energy*, vol. 48, no. 6. 2023. doi: 10.1016/j.ijhydene.2022.10.058.

[15] B. Hasanah, "Studi Tingkat Kerusakan Bangunan Rumah Terhadap Serangan Rayap Di Kecamatan Bankit Kabupaten Way Kanan," *Fakultas Tarbiyah Dan Keguruan IAIN Raden Intan Lampung*, 2021.

[16] N. Alhazmi, D. B. Ingham, M. S. Ismail, K. J. Hughes, L. Ma, and M. Pourkashanian, "Effect of the anisotropic thermal conductivity of GDL on the performance of PEM fuel cells," *Int J Hydrogen Energy*, vol. 38, no. 1, pp. 603–611, Jan. 2013, doi: 10.1016/j.ijhydene.2012.07.007.

[17] A. Martín-Alcántara, L. González-Morán, J. Pino, J. Guerra, and A. Iranzo, "Effect of the Gas Diffusion Layer Design on the Water Management and Cell Performance of a PEM Fuel Cell," *Processes*, vol. 10, no. 7, 2022, doi: 10.3390/pr10071395.

[18] M. Kaplan, "Numerical investigation of influence of cross-sectional dimensions of flow channels on pem fuel cell performance," *Journal of Energy Systems*, vol. 5, no. 2, 2021, doi: 10.30521/jes.871018.

[19] E. E. Kahveci and I. Taymaz, "Assessment of single-serpentine PEM fuel cell model developed by computational fluid dynamics," *Fuel*, vol. 217, 2018, doi: 10.1016/j.fuel.2017.12.073.

[20] A. Biyikoğlu and C. Ö. Alpat, "Parametric study of a single cell proton exchange membrane fuel cell for A bundle of straight gas channels," *Gazi University Journal of Science*, vol. 24, no. 4, 2011.

[21] C. Spiegel, *PEM Fuel Cell Modeling and Simulation Using Matlab*. 2008. doi: 10.1016/B978-0-12-374259-9.X5001-0.

[22] F. Barbir, *PEM fuel cells: Theory and practice*. 2012. doi: 10.1016/C2011-0-06706-6.